First-principles calculation of the Coulomb pseudopotential μ^* for the simple hexagonal phase of Si

1997 J. Phys.: Condens. Matter 9 6351

(http://iopscience.iop.org/0953-8984/9/30/004)

J. Phys.: Condens. Matter **9** (1997) 6351–6358. Printed in the UK PII: S0953-8984(97)83463-7

First-principles calculation of the Coulomb pseudopotential μ^* for the simple hexagonal phase of Si

Young-Gu Jin, K-H Lee and K J Chang

Department of Physics, Korea Advanced Institute of Science and Technology, 373-1, Kusung-dong, Yusung-ku, Taejon, Korea

Received 15 April 1997, in final form 29 May 1997

Abstract. We calculate the Coulomb pseudopotential μ^* for the simple hexagonal phase of Si at a pressure of 14 GPa using a full-dielectric-matrix approach within the local-density-functional approximation. With all of the screening effects such as the crystal potential, local-field, and exchange–correlation effects, the value of μ^* is estimated to be 0.104. Considering only the crystal potential effect, μ^* is found to be very close to that of a free-electron gas. The exchange–correlation effect on the electron dielectric response function decreases the dielectric screening, especially for large wave vectors, giving rise to an increase of μ^*, while the local-field effect which results from directional bonds slightly reduces μ^*.

Si undergoes a sequence of structural phase transitions with increasing pressure; a semiconducting diamond phase changes into a metallic β-Sn phase at about 10 GPa, and then transforms into a simple hexagonal (sh) phase at about 13 GPa [1–6]. With further increase of pressure, successive structural transformations into highly coordinated compact structures such as hexagonal-close-packed (hcp) and face-centred-cubic (fcc) structures occur [1–3]. All of the metallic phases were shown to be superconducting at low temperatures [7–11], while the superconductivity of the fcc phase was only predicted theoretically [12]. In the β-Sn and sh phases, the superconducting temperatures (T_c) were found to be fairly high, 6.3 and 8.2 K at 12 and 15.2 GPa, respectively [7]. Since the sh phase has both interlayer covalent-like bonds and intralayer metallic bonds, this structure has soft transverse acoustic (TA) phonon modes along the [001] direction, which vary sensitively with pressure and induce a phase transformation into the hcp structure [4, 6]. Because of the directional bonds and soft phonon modes [7–9], the sh phase was shown to have stronger electron–phonon couplings and higher T_c-values, as compared to other β-Sn and hcp phases, although the density of states at the Fermi level is comparable to that of a free-electron gas. To determine T_c, it is necessary to estimate both the electron–phonon coupling (λ) and the electron–electron Coulomb repulsion, which is usually represented by μ^*. It is now possible to calculate both of the parameters λ and μ^* from first principles [13–16]. In previous work for sh Si [7, 9], the electron–phonon couplings were calculated for particular phonons along high-symmetry directions in the Brillouin zone (BZ); however, a spherical average of the momentum-dependent electron–phonon couplings for the BZ summation was used to determine λ. Thus, knowing the exact value of μ^* is essential for checking the reliability of the methods of calculation for λ.

In this work, we calculate the Coulomb pseudopotential μ^* for Si in the simple hexagonal phase using a first-principles pseudopotential method within the local-density-functional approximation (LDA) [17]. Based on the full-dielectric-matrix approach which includes

0953-8984/97/306351+08$19.50

crystal-field, local-field, and exchange–correlation effects, the value of μ^* is estimated to be 0.104 for the sh phase at a pressure of 14 GPa. With only the crystal potential effect, μ^* is found to be 0.100, which is nearly equal to that of a free-electron gas. We find that the local-field effect which results from the interlayer covalent bonds slightly decreases the Coulomb repulsion parameter, while the exchange–correlation effect on the electron dielectric screening significantly increases μ^*. Our calculated value for μ^* is expected not to change drastically with pressure, because the density of states at the Fermi level is not sensitive to the variation of pressure, although λ was shown to vary significantly with pressure due to soft TA phonon modes [7–9].

In analogy with the electron–phonon coupling parameter λ, the Coulomb repulsive interaction between electrons of a Cooper pair is expressed by the repulsion parameter μ, defined as the Fermi-surface average of the instantaneous screened electron–electron interaction [18]:

$$\mu = N(0)\langle\langle V^c_{n\boldsymbol{k},n'\boldsymbol{k}'}\rangle\rangle_{FS} \tag{1}$$

where $N(0)$ is the density of states per spin at the Fermi energy ε_F, $\langle\langle\ \rangle\rangle_{FS}$ denotes the Fermi-surface average, and $V^c_{n\boldsymbol{k},n'\boldsymbol{k}'}$ is the Coulomb scattering matrix element of a Cooper pair from a state $|n\boldsymbol{k}, n-\boldsymbol{k}\rangle$ to $|n'\boldsymbol{k}', n'-\boldsymbol{k}'\rangle$:

$$V^c_{n\boldsymbol{k},n'\boldsymbol{k}'} = \int \mathrm{d}\boldsymbol{r}\ \mathrm{d}\boldsymbol{r}'\ \psi^*_{n'\boldsymbol{k}'}(\boldsymbol{r})\psi^*_{n'-\boldsymbol{k}'}(\boldsymbol{r}')V^c(\boldsymbol{r},\boldsymbol{r}')\psi_{n\boldsymbol{k}}(\boldsymbol{r})\psi_{n-\boldsymbol{k}}(\boldsymbol{r}'). \tag{2}$$

Here the screened Coulomb potential $V^c(\boldsymbol{r},\boldsymbol{r}')$ is expressed in terms of the inverse dielectric function ϵ^{-1} and the bare Coulomb potential V^c_{bare}:

$$V^c(\boldsymbol{r},\boldsymbol{r}') = \int \mathrm{d}\boldsymbol{r}''\ \epsilon^{-1}(\boldsymbol{r},\boldsymbol{r}'')V^c_{\mathrm{bare}}(\boldsymbol{r}'',\boldsymbol{r}'). \tag{3}$$

In the case of phonon-mediated superconductivity, the Coulomb repulsion parameter μ is rescaled to μ^* due to retardation effects, which are caused by the difference between the phononic and electronic cut-off energies [19, 20]. Assuming a constant Coulomb scattering kernel up to the Fermi energy, μ^* is written as

$$\mu^* = \frac{\mu}{1+\mu\ln(\varepsilon_F/\Theta_D)} \tag{4}$$

where Θ_D is the Debye energy representing the cut-off energy of the phonon-induced interaction.

To calculate the repulsion parameter μ in equation (1), the electron wave functions and band energies are generated by the first-principles pseudopotential method within the LDA. Norm-conserving pseudopotentials are generated by the scheme of Hamann, Schlüter, and Chiang [21]. The Wigner interpolation formula is used for the exchange–correlation potential [22]. The valence wave functions and the dielectric matrix are expanded in a plane-wave basis set with a kinetic energy cut-off of 12 Ryd. The Brillouin zone summations are performed using a uniform grid of 84 $\boldsymbol{k}$-points in the irreducible sector of the BZ. Testing the kinetic energy cut-off of 16 Ryd and a grid of 252 $\boldsymbol{k}$-points, we find the bulk properties of simple hexagonal Si to be well converged. The total energies for the sh phase are optimized by varying the axial ratio, and are fitted to the Murnaghan's equation of state [23]. At 14 GPa, the crystal volume and the axial ratio c/a are estimated to be 13.41 Å^3 per atom and 0.939, respectively. The density of states and the Fermi energy are calculated by the linear tetrahedron method [24] with a set of 84 $\boldsymbol{k}$-points in the irreducible BZ. The linear tetrahedron method with 84 $\boldsymbol{k}$-points is also used for the Fermi-surface integration in equation (1). For the Thomas–Fermi screening function, we find that the errors of the

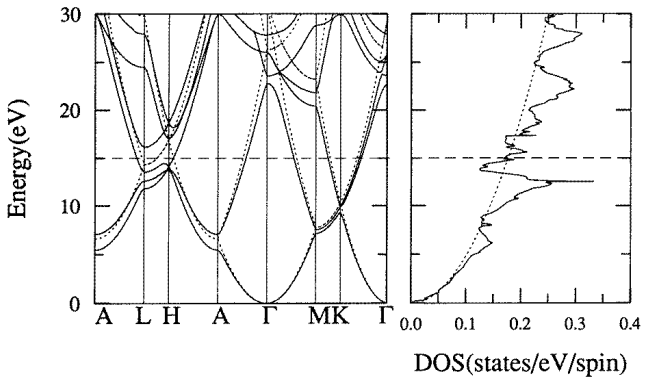

Figure 1. The band structure and DOS of sh Si are drawn for a crystal volume of 13.41 Å^3/atom with the axial ratio $c/a = 0.939$. The horizontal line denotes the Fermi level, and the dotted curves represent the free-electron band.

dielectric matrix elements are less than 5%, by increasing the number of $\boldsymbol{k}$-points up to 440 points, leading to the negligible change of μ.

The calculated band structure and density of states (DOS) for the sh phase are plotted in figure 1. The Fermi energy ε_F and the density of states at ε_F are calculated to be 15.02 eV and 0.172 states eV^{-1} per spin, respectively, as compared to the values of 16.28 eV and 0.184 states eV^{-1} per spin obtained from the free-electron-gas model. Overall, the band structure for energies below ε_F is similar to that of the free-electron model, while the lowest four bands along the LH direction of the BZ, which are split by the crystal potential, are different. The lowest three levels along the LH direction give rise to a large peak in the DOS at $\varepsilon_F - 0.5$ eV. We find that this feature is not much changed at higher pressures. Because no state crosses the Fermi level on the LH axis, the calculated value of $N(0)$ is slightly smaller than that of the free-electron model.

The dielectric response function is calculated in momentum space, using the perturbative approach based on the LDA [17, 25]. For a weak external potential $\delta\phi_{ext}$, the total internal potential change is $\delta\phi_{tot} = \epsilon^{-1}\delta\phi_{ext}$ in the abbreviated form. The inverse of the dielectric matrix (IDM) can be derived by calculating the full polarizability χ, which is related to the independent-particle polarizability χ_0 by $\chi = (1 - \chi_0 V^c_{\text{bare}} - \chi_0 K_{xc})^{-1}\chi_0$ [25]. Here K_{xc} is the functional derivative of the exchange–correlation potential, and χ_0 is directly obtained in terms of the single-particle wave functions and the eigenvalues of the unperturbed Hamiltonian [26]. The off-diagonal elements of the dielectric matrix, which constitute the so-called local-field effect, represent the inhomogeneous distribution of electron charge. In the interacting electron gas, the local-field factor $G(q)$ is often used for the exchange–correlation effect, and in our calculations this factor is related to $K_{xc} = -V^c_{\text{bare}}G(q)$. Depending on the probe of the response, two different dielectric response functions can be defined [25]; if the probe is a test charge, the so-called test-charge (TC) dielectric function is given by $\epsilon^{-1}_{TC} = 1 + V^c_{\text{bare}}\chi$; if the probe is constituted by the electrons themselves, the exchange–correlation interaction between the probe and the induced charge is additionally included in the screening, and, then, the electron dielectric function is expressed as $\epsilon^{-1}_{el} = 1 + (V^c_{\text{bare}} + K_{xc})\chi$. We test both of the dielectric functions, ϵ^{-1}_{TC} and ϵ^{-1}_{el}, and find that ϵ^{-1}_{el} is generally enhanced, as compared to ϵ^{-1}_{TC}. For a Cooper pair, since electrons are treated as the probe, it is more appropriate to choose the electron dielectric function for the screening between the electrons [16].

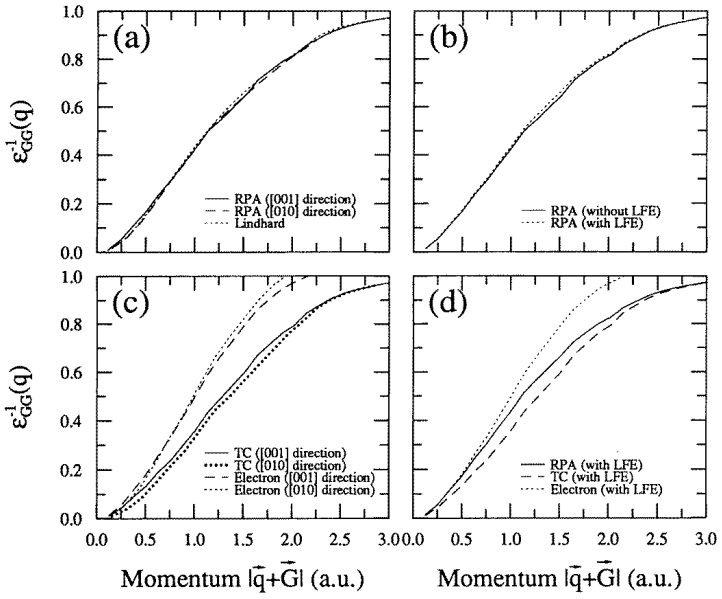

Figure 2. The diagonal elements of the static inverse dielectric matrices. In (a), without the local-field effect, the RPA dielectric functions are compared with the Lindhard functions along the [001] and [010] directions. The RPA dielectric functions with and without the local-field effect along the [001] direction are compared in (b). In (c), with the local-field effect (LFE), the TC and electron dielectric functions are compared along the [001] and [010] directions, while in (d) the RPA, TC, and electron dielectric functions are plotted along the [001] direction.

In the random-phase approximation (RPA), where the exchange–correlation interaction is ignored, the dielectric screening is found to be similar to the Lindhard dielectric screening, as shown in figure 2(a). In this case, since the difference between the RPA screenings along two different crystal directions, [001] and [010], is very small, the crystal-field effect is considered to be extremely small. When we include the local-field effect which results from inhomogeneous charge distributions, the diagonal elements of the static IDM, $\epsilon^{-1}_{GG}(\boldsymbol{q})$, are increased by about 5%, as shown in figure 2(b). With the RPA dielectric matrix, we investigate the screened Coulomb potential around a point charge $-e$ at $\boldsymbol{r}'$ with a test probe $-e$ at $\boldsymbol{r}$ in equation (3). Figure 3 shows the change of the screened potential from the bare Coulomb potential caused by the local-field effect for two cases, where the test probes are located at two different bond-centred sites of the interlayer and intralayer bonds. Since the axial ratio of sh Si was shown to be smaller than one, the interlayer bonds were considered to be more covalent than those on the hexagonal planes, and these bonds have more accumulations of the valence electrons, Thus, we find that the electrostatic screening of the Coulomb potential generated by the added charge in the interlayer bond is more effective. This feature is well reflected by the off-diagonal elements of the IDM, as illustrated in figure 3.

On including the exchange–correlation interaction in the dielectric screening (see figure 2(c)), we find that the electron $\epsilon^{-1}_{GG}(\boldsymbol{q})$s are larger than the RPA ones, especially for large wave vectors, while the test-charge $\epsilon^{-1}_{GG}(\boldsymbol{q})$s are smaller. The same screening effect of the exchange–correlation interaction was also found for Nb [16]. The enhancement of the inverse of the electron dielectric matrix was attributed to the decrease of the screening, which

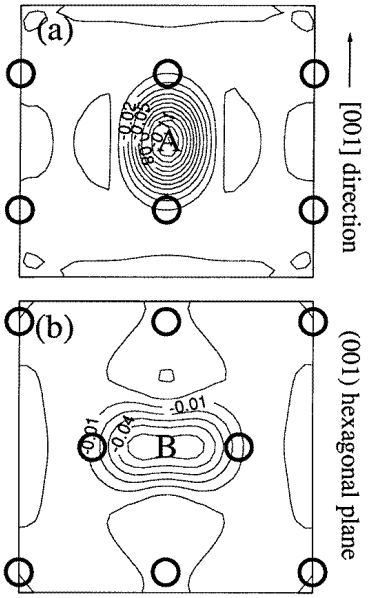

Figure 3. The equipotential lines for the change of the Coulomb potential by the local-field effect are plotted for two added charges located at the interstitial sites A and B, which are in the (a) intralayer and (b) interlayer bonds on the (010) and (001) planes, respectively. Circles denote the Si atoms, and contour spacings are in atomic units.

results from a deficiency of the induced charge around the probe [16]. Since the exchange–correlation contribution K_{xc} has a short-range character, the reduction of screening in the electron dielectric function is more significant for large momenta. However, it should be noted that this reduction of screening is slightly exaggerated in the region of large momentum, because of the use of the LDA K_{xc}, which is independent of momentum. In the case of the TC dielectric function, the exchange–correlation interaction effectively increases the induced charge; then, the Coulomb interaction between the probe and the induced charge results in more screening.

As discussed earlier, the RPA $\epsilon^{-1}_{\boldsymbol{GG}}(\boldsymbol{q})$s are very similar for wave vectors along two high-symmetry [001] and [010] directions, except for in the region of small wave vectors, where the screening along the [001] axis is slightly smaller than that along the [010] direction. This difference is reflected by weak crystal fields, which also broaden the band structure, particularly along the LH direction. However, if we consider the exchange–correlation interaction, we find that the screening effect depends more clearly on the direction of $\boldsymbol{q}$ (see figure 2(c)). For the TC dielectric matrix, the magnitudes of the $\epsilon^{-1}_{\boldsymbol{GG}}(\boldsymbol{q})$s are found to be larger over the whole range of wave vectors along the [001] direction. On the other hand, since the electron $\epsilon^{-1}_{\boldsymbol{GG}}(\boldsymbol{q})$s are similar to the RPA ones in the small-momentum region, their magnitudes along the [001] direction are larger for small wave vectors. In this case, although the screening effect is more significant for large wave vectors on the [001] axis than that on the [010] axis, their difference might be slightly exaggerated because the LDA exchange–correlation potential is used. Since the local-field effect depends directly on the directionality of bonds, its contribution to the dielectric screening is larger for wave vectors along the [001] direction, where covalent-like interlayer bonds are formed, while the intralayer bonds on the (001) hexagonal planes are metallic.

Table 1. The calculated values for μ and μ^* are given for the Lindhard, RPA, TC, and electron dielectric screenings. The Debye temperature Θ_D is chosen to be 550 K (reference [27]).

	Lindhard	RPA	TC	Electron
Without the local-field effect				
μ	0.235	0.238	0.200	0.274
μ^*	0.100	0.100	0.093	0.106
With the local-field effect				
μ		0.225	0.186	0.261
μ^*		0.098	0.090	0.104

In table 1, the calculated values for μ and μ^* are listed for the Lindhard, RPA, TC, and electron dielectric screenings. For the free-electron system, one can estimate the exact value of 0.230 for μ from the following expression [28]:

$$\mu = \frac{N(0)}{2} \int_0^{2k_F} \frac{4\pi e^2 \, \mathrm{d}q}{q {k_F}^2 \epsilon_{\mathrm{free}}(q)} \tag{5}$$

where k_F is the Fermi wave vector, and $\epsilon_{\mathrm{free}}(q)$ is the free-electron dielectric function. To calculate the Fermi-surface average of $V^c_{n\boldsymbol{k},n'\boldsymbol{k}'}$ in equation (2), we use the linear tetrahedron method for all of the dielectric screenings considered here. In the case of the Lindhard function, we obtain the value of 0.235 for μ, resulting in $\mu^* = 0.100$, in good agreement with the value directly estimated from equation (5). For the RPA dielectric screening without the local-field effect, the calculated values of μ and μ^* are found to be very similar to those for the Lindhard function, as expected from figure 2(a). When the local-field effect is included, μ is generally reduced by 5–7%, and similar behaviour was also found for Al and Nb [15, 16]. On the other hand, the exchange–correlation effect increases μ by about 15% for the electron dielectric screening, as compared to the RPA dielectric function. Although the local-field and exchange–correlation effects compete with each other, the exchange–correlation contribution is more significant, and compensates for the decrease of μ by the local-field effect. In the case of the TC dielectric function, since the exchange–correlation effect enhances the dielectric screening, μ is reduced by about 16–17%, regardless of whether the local-field effect is included or not. Including the full screening effects, μ^* is calculated to be 0.104 for the electron dielectric function. This estimate is close to the value of 0.10 used in most theoretical calculations to determine the superconducting transition temperatures of simple metals. Although the electron–phonon coupling has a large dependence on covalent-like interlayer bonds [7, 9], the dielectric screenings are not seriously influenced by these.

The electron–phonon coupling constant λ can be determined by taking the average of the λ_qs over the entire BZ [7, 13, 29, 30]:

$$\lambda = \frac{1}{\Omega_{BZ}} \int \lambda_{\boldsymbol{q}} \, \mathrm{d}\boldsymbol{q} \tag{6}$$

where Ω_{BZ} is the volume of the Brillouin zone, and $\lambda_{\boldsymbol{q}}$ is the sum of all of the phonon branches at $\boldsymbol{q}$. For sh Si, the electron–phonon coupling constant λ was first calculated using the first-principles pseudopotential method [7]. In this work, only the [001] direction was considered, and the average λ of about 0.4 at a pressure around 13 GPa was obtained using a spherical approximation to the average in equation (6). From the McMillan equation for T_c [31], with the use of $\mu^* = 0.104$, $\Theta_D = 550$ K, and $T_c \sim 7.5$ K, we estimate λ to be about 0.55. Thus, the use of just the [001] direction for obtaining the average λ seems to

lead to an underestimate of λ, indicating a shortcoming of the calculation. This feature was recognized in later calculations, which showed that, for other high-symmetry directions, the electron–phonon interaction for the $\boldsymbol{q}$s along the [011] direction is very different from that for the $\boldsymbol{q}$s along the [001] axis, and exhibits a large enhancement of λ [11]. The increase of λ is caused by the soft transverse mode in the sh phase, which is associated with the structural transformation from sh Sn to β-Sn. Although it is expected that a full average in equation (6) will give a better agreement with the one estimated from our present calculations for μ^*, a complete comparison of λ requires more accurate calculations of $\lambda_{\boldsymbol{q}}$ over the whole Brillouin zone.

In conclusion, we have calculated the Coulomb pseudopotential μ^* for Si in the simple hexagonal phase using the first-principles pseudopotential method. Considering all of the screening effects, the resulting μ^* is estimated to be 0.104. The RPA value of μ^* without the local-field effect is found to be very similar to that of the free-electron gas, demonstrating that the crystal-field effect is very small. The local-field effect resulting from the interlayer covalent bonds increases the dielectric screening, and thus μ^* is slightly decreased. However, with the exchange–correlation effect, the electron screening is enhanced, resulting in the increase of μ^*.

Acknowledgments

This work was supported by the MOST, KOSEF and the CMS at the Korea Advanced Institute of Science and Technology.

References

[1] Hu J Z and Spain I L 1984 *Solid State Commun.* **51** 263
[2] Olijnyk H, Sikka S K and Holzapfel W B 1984 *Phys. Lett.* **103A** 137
[3] Duclos S J, Vohra Y K and Ruoff A L 1990 *Phys. Rev.* B **41** 12 021
[4] Chang K J and Cohen M L 1984 *Phys. Rev.* B **30** 5376
[5] Needs R J and Martin R M 1984 *Phys. Rev.* B **30** 5390
[6] Chang K J and Cohen M L 1985 *Phys. Rev.* B **31** 7819
[7] Chang K J, Dacorogna M M, Cohen M L, Mignot J M, Chouteau G and Martinez G 1985 *Phys. Rev. Lett.* **54** 2375
[8] Chang K J and Cohen M L 1986 *Phys. Rev.* B **34** 4552
[9] Dacorogna M M, Chang K J and Cohen M L 1985 *Phys. Rev.* B **32** 1853
[10] Mignot J M, Chouteau G and Martinez G 1986 *Phys. Rev.* B **34** 3150
[11] Erskine D E, Yu P Y, Chang K J and Cohen M L 1986 *Phys. Rev. Lett.* **57** 2741
[12] Liu A Y, Chang K J and Cohen M L 1988 *Phys. Rev.* B **37** 6344
[13] Cohen M L, Chang K J and Dacorogna M M 1985 *Physica* B **135** 229
[14] Savrasov S Y, Savrasov D Y and Andersen O K 1994 *Phys. Rev. Lett.* **72** 372 and references therein
[15] Lee K-H, Chang K J and Cohen M L 1995 *Phys. Rev.* B **52** 1425
[16] Lee K-H and Chang K J 1996 *Phys. Rev.* B **54** 1419
[17] Kohn W and Sham L J 1965 *Phys. Rev.* **140** A1133
[18] Allen P B and Mitrović B 1982 *Solid State Physics* vol 37 (New York: Academic) p 25
[19] Morel P and Anderson P W 1962 *Phys. Rev.* **125** 1263
[20] Bogoliubov N N 1958 *Nuovo Cimento* **7** 794
[21] Hamann D R, Schlüter M and Chiang C 1979 *Phys. Rev. Lett.* **43** 1943
[22] Wigner E 1938 *Trans. Faraday Soc.* **34** 678
[23] Murnaghan F D 1944 *Proc. Natl Acad. Sci. USA* **30** 244
[24] Lehmann G and Taut M 1972 *Phys. Status Solidi* b **54** 409
[25] Hybertsen M S and Louie S G 1987 *Phys. Rev.* B **35** 5585
Hybertsen M S and Louie S G 1987 *Phys. Rev.* B **35** 5602
[26] Adler S L 1962 *Phys. Rev.* **126** 413

Wiser N 1963 *Phys. Rev.* **129** 62
[27] With the maximum longitudinal acoustic phonon frequency as the cut-off in the phonon spectrum (see reference [7]), we estimate the Debye temperature to be 550 K.
[28] Grimvall G 1981 *The Electron–Phonon Interaction in Metals* (Amsterdam: North-Holland)
[29] Dacorogna M M and Cohen M L 1985 *Phys. Rev. Lett.* **55** 83
[30] Lam P K, Dacorogna M M and Cohen M L 1986 *Phys. Rev.* B **34** 5065
[31] McMillan W L 1968 *Phys. Rev.* **167** 331